ELSEVIER

Chemistry and Physics of Lipids
104 (2000) 193–206

CPL
CHEMISTRY AND PHYSICS OF LIPIDS

www.elsevier.com/locate/chemphyslip

Cholesterol-induced alterations of the packing properties of gangliosides: an EPR study

M.M. Pincelli [a], P.R. Levstein [a], G.D. Fidelio [b], A.M. Gennaro [c,*]

[a] *Facultad de Matemática, Astronomía y Física, Universidad Nacional de Córdoba, Ciudad Universitaria, 5000 Córdoba, Argentina*
[b] *Departamento de Química Biológica — CIQUIBIC, Facultad de Ciencias Químicas, Universidad Nacional de Córdoba, Ciudad Universitaria, 5000 Córdoba, Argentina*
[c] *INTEC (CONICET) and Facultad de Bioquímica y Ciencias Biológicas, Universidad Nacional del Litoral, Güemes 3450, 3000 Santa Fe, Argentina*

Received 28 May 1999; received in revised form 18 October 1999; accepted 18 October 1999

Abstract

The effect of cholesterol (Chol) on two kinds of glycolipid assemblies, one composed of monosialogangliosides (G_{M1a}) and the other formed by a natural mixture of bovine brain gangliosides (TBG), has been analysed. The experimental approach involves spin label electron paramagnetic resonance (EPR) in aqueous lipid dispersions. The employment of a hydrosoluble spin label and a 'quencher' of the EPR signal that is not able to permeate lipid interfaces, allowed us to conclude that G_{M1a}/Chol mixtures give rise to vesicles at Chol proportions for which TBG/Chol mixtures form micelles. The use of different liposoluble spin labels reveals that cholesterol produces a straightening of the hydrocarbon chains in both lipid systems. In G_{M1a}/Chol mixtures, this feature is more pronounced and it is coupled with a decrease in polarity at the chain ends.

Keywords: Glycolipids; Lipid polymorphism; Supramolecular aggregates; Micelles; Vesicles; Spin labels

1. Introduction

The types of supramolecular structures formed by amphiphiles are determined by a complex balance of attraction and repulsion between the molecules, including interactions with the solvent and entropic effects. However, if one assumes that no water can occupy the hydrophobic region, the supramolecular structure of the aggregates can be approximately predicted by considering the 'schematic shapes' associated with the different molecules that constitute the building blocks. Thus, lipids having a cone shape form micelles, those having a cylinder or truncated cone shape form bilayers, and those having a wedge shape tend to form inverted hexagonal II structures (Israelachvili, 1991). The presence of a rigid

* Corresponding author. Fax: +54-342-4550944.
E-mail address: agennaro@intec.unl.edu.ar (A.M. Gennaro)

0009-3084/00/$ - see front matter
PII: S0009-3084(99)00127-9

molecule like cholesterol can originate new different structures (Perkins et al., 1997). For instance, the cone shaped lysophosphatidylcholine, when mixed with cholesterol at a certain molar ratio, forms bilayer structures (Kumar et al., 1988).

We have a project to study correlations between lipid composition, structure and dynamics of biologically relevant supramolecular aggregates related to membranes. In particular, we are interested in the properties that the carbohydrate rich lipids impose to these aggregates.

Gangliosides are double-tailed glycosphingolipids containing residues of sialic acid in their large oligosaccharide polar headgroup. They are concentrated in the outer hemilayer of animal plasma cell membranes, especially of nerve tissue. Their presence is related to processes taking place at the cell surface such as adhesion, membrane fusion, membrane mediated transfer of information, recognition of enzymes, etc. (Ledeen et al., 1988; Maggio, 1994; Simons and Ikonen, 1997). The gangliosides composing the natural mixture in the bovine brain, henceforth called total brain gangliosides (TBG), are cone shaped. It has been shown that, in aqueous media, each of the gangliosides forming the TBG natural mixture self-assembles in micelles with CMC in the range 10^{-9}–10^{-7} M (Tettamanti and Masserini, 1987; Cantù et al., 1997). Only when there are very few water molecules (≈ 150) per ganglioside molecule, a transition to hexagonal I phase occurs. On the other hand, it was also proved that at physiological pH the TBG equilibrium state involves a perfect mixture of all the components (Liu and Chan, 1991). Thus, it is reasonable to predict the formation of micelles in aqueous solutions of TBG above the CMC.

In a previous work, we found by using nuclear magnetic resonance of phosphorus (^{31}P-NMR) that the addition of TBG to vesicles of phosphatidylcholine (PC) reduces their radii of curvature, leading to the collapse of the bilayer and the formation of micelles and small aggregates (Pincelli et al., 1998). We also observed that this process is partially reversed by the addition of cholesterol (Chol), which stabilises the bilayer structure. It is known that the cholesterol molecule behaves as if it were a wedge, but in water dispersions, only under very restrictive conditions it is able to form rod-like micelles (Castanho et al., 1992). Otherwise, it does not form by itself any of the mentioned structures (Carnie et al., 1979). When added to phospholipid membranes, Chol weakens the Van der Waals interactions between lipids fluidifying the bilayer structure in its gel phase, but rigidifying it in the liquid crystalline state by restricting the *trans-gauche* isomerisations (Van der Meer, 1993). Thus, Chol broadens the gel to liquid-crystalline phase transition. On another side, there are not systematic studies on the ganglioside-cholesterol binary system. The interactions in this system have become a very important issue, since recent findings indicate that in certain cells sphingolipids and Chol segregate in dynamic clusters that move within the fluid bilayer. These 'rafts' can bind proteins, and it has been proposed their participation in signal transduction (Simons and Ikonen, 1997). A recent work (Bagatolli et al., 1998) reports the effect of the addition of 20% Chol to some gangliosides on the dynamical properties of the water associated with the aggregates. This study was carried out using an amphiphilic fluorescence probe and the results seem to indicate a cholesterol-induced dehydration of the interface in the gel phase. This effect decreases with the size of the polar headgroups, suggesting that it depends on the curvature radius as well as on the extent of hydration of the lipid aggregate. However, to our knowledge, the topology of the aggregates formed by gangliosides and Chol has not been reported until now. In this work, we investigate the types of structures formed by mixtures ganglioside/Chol dispersed in water over a wide range of composition. The gangliosides studied are monosialogangliosides (G_{M1a}) and TBG.

2. Materials and methods

2.1. Materials

Gangliosides from bovine brain were purified to better than 99% as described elsewhere (Fidelio et al., 1991). G_{M1a} is a monosialoganglioside, and the natural mixture TBG contains 21% G_{M1a}, 60%

spin labels were the liposoluble n-doxyl stearic acid positional isomers (n-SASL, $n = 5$, 12 and 16) and the water soluble tempamine (4 amino-tempo, TA). The spin labels, cholesterol and Tris buffer, were purchased from Sigma (St Louis, MO). Potassium ferricyanide ($K_3Fe(CN)_6$) was used as a quencher of the EPR signal. All chemicals were of analytical reagent grade.

2.2. Sample preparation

Stock solutions of lipids in organic solvents were prepared. Chol was dissolved in chloroform/methanol (2:1 v/v), and gangliosides in chloroform/methanol/0.01 N NaOH (60:30:4.5). To prepare lipid dispersions at different molar ratios, appropriate aliquots of stock solutions were mixed. Then, the organic solvent was evaporated with a stream of dry nitrogen and the lipids were kept under vacuum overnight. The dry lipids (5 μmol in total) were dispersed in 50 μl of Tris buffer (50 mM, pH 7.2). The dispersion was vortexed and heated in a thermal bath to 55–60°C during an hour in order to ensure complete hydration. Chol partial molar content, related to total lipids, is indicated by x_{Chol}.

After lipid hydration, it was observed that the aqueous dispersions of pure G_{M1a} and TBG are transparent. TBG/Chol mixtures remain completely transparent up to $x_{Chol} = 0.3$, looking somewhat turbid at higher Chol proportions. From the turbid TBG/Chol samples it was possible to obtain a pellet after centrifugation. Thin layer chromatography of the separated pellets and supernatants showed that both portions contain gangliosides and cholesterol in similar ratios. This fact guarantees that at these proportions ($x_{Chol} \leq 0.5$) there is no cholesterol segregation. G_{M1a}/Chol mixtures present a slight turbidity at $x_{Chol} = 0.2$ and, as x_{Chol} increases, this characteristic is more pronounced.

2.3. Spin labelling

TBG and G_{M1a} samples with $x_{Chol} = 0.0$, 0.3 and 0.5 were labelled with the water-soluble spin label tempamine (TA), and samples with $x_{Chol} =$ 0.0, 0.1, 0.2, 0.3, 0.4 and 0.5 were studied with the liposoluble n-SASL ($n = 5$, 12 and 16). The TA label was dissolved in buffer and incorporated when the lipids were dispersed, to a final TA concentration of 1 mM. It was checked that for concentrations below 2 mM, the TA spectra are not broadened by spin–spin interactions. It was also checked that the thermal treatment does not degrade the spin labels, as EPR spectra from samples in which TA was added after the hydration process showed no differences with those from samples subject to the regular treatment. In the experiments with liposoluble spin labels, 1 mol% of the required n-SASL, previously dissolved in ethanol, was added when the lipids were mixed.

2.4. EPR spectroscopy

The EPR spectra were recorded at (25 ± 1)°C and 9.8 GHz (X Band) in a ER-200 spectrometer (Bruker Analytische Messtechnik GMBH, Karlsruhe, Germany). The samples were placed in glass capillaries (1 mm i.d.), sealed at both ends and housed in 4-mm quartz tubes containing silicone oil for maintaining temperature uniformity. Field modulation frequency was 100 KHz, and its amplitude was well below 30% of the minor linewidths in each case, to avoid spectral shape distortions.

2.5. Characterisation of the aggregates

The differentiation between micelles and vesicles involves the use of a hydrophilic spin label which must be distributed over all the aqueous environments, and a quencher of the EPR signal that does not permeate lipid interfaces. Thus, comparison of the EPR signals before and after quenching yields direct information about the presence of water enclosing aggregates. Further procedures leading to the equilibration of inner and outer aqueous media give conclusive evidence about the origin of the signal after quenching, as detailed below.

2.5.1. Experimental protocol

The water-soluble spin label TA, which is positively charged at the working pH value, was in-

corporated simultaneously with the buffer used to swell the lipids. In these conditions, this label does not partition into the hydrophobic region of lipids (Sunamoto et al., 1992). Thus, TA is expected to be in the aqueous bulk, in water enclosed by vesicles, and/or near the negatively charged sialic acids at the ganglioside polar headgroups.

Subsequent quenching of the EPR signal originated in the bulk TA spin label is performed by adding potassium ferricyanide up to a final concentration of at least 65 mM. The quenching effect of this concentration of ferricyanide anion $[Fe(CN)_6]^{3-}$ (FCN) on a 1-mM TA solution in buffer was checked, and the quenched spectrum has an amplitude well below 0.5% of the unquenched one. A broad residual three-line structure, detected only upon amplification, remains in the quenched spectrum. Although a less structured line is obtained after quenching with more concentrated FCN solutions, the lowest concentration minimises changes in the ionic strength during the quenching procedure. In order to facilitate the interpretation of quenched spectra in relevant samples, the 1-mM TA spectrum in pure buffer, quenched with 65 mM FCN, will be displayed in the same scale in the corresponding figures.

FCN is a fast relaxing agent that quenches reversibly only the signals of those TA molecules in its close proximity, and it does not permeate lipid interfaces (Morse, 1986; Sunamoto et al., 1992). Thus, in quenched samples the EPR signals should be ascribed to TA in the aqueous medium enclosed by vesicles, or kept by electrostatic interactions in protected sites among the ganglioside headgroups.

To identify the signals coming from confined water, a further freeze-and-thaw procedure (F&T) was performed. Quenched samples were submerged alternatively (five times) in liquid nitrogen and in warm water, allowing for thermal equilibration at each step of the cycle. This procedure causes the destruction and reassemble of the lipid structures and consequently, a complete equilibration of the inner and outer aqueous media (Mayer et al., 1985), allowing the FCN ions to quench the spectrum of the TA molecules dissolved in the inner medium. Therefore, any eventual EPR signal should only come from those TA molecules that are able to remain in protected sites in the ganglioside headgroup region.

For each of the lipid dispersions, we studied a set of three samples. The 'original' sample, separated before the addition of FCN, the 'quenched' sample, separated after the addition of FCN, and the 'F&T' sample, an aliquot of the quenched sample submitted to the F&T procedure. TBG and G_{M1a} aggregates with $x_{Chol} = 0.0$, 0.3 and 0.5 were studied in this way.

2.5.2. Analysis of the EPR spectra

The information available from the EPR spectra of TA is based on well-established correlations (Griffith and Jost, 1976):

- the isotropic ^{14}N-hyperfine coupling constant A_0 gives information about the micropolarity of the label environment, increasing with polarity;
- the correlation time τ_c is proportional to the microviscosity of the environment of the label (Morse, 1986; Gennaro et al., 1996); and
- the intensity of the signal I_0 reflects the relative amount of label not accessible to FCN.

In our samples, the spectra of the TA label show narrow equally-spaced lines, indicative of a highly mobile species in a low viscosity regime (Wertz and Bolton, 1972). In this case, the hyperfine constant A_0 is obtained from the difference (in Gauss) between the low and high-field lines $2A_0$.

In this regime, the Debye formula $\tau_c = V_h \eta / kT$, where V_h is the hydrodynamic volume of the spin label and k the Boltzmann constant, relates the rotational correlation time of the label with the microviscosity η of the environment at a given temperature T. Then, the environment microviscosity relative to that of the buffer can be calculated as $\eta_r = \eta/\eta_{buffer} = \tau_c/\tau_{c\ buffer}$. τ_c (in seconds) is calculated according to the standard formula for isotropic high mobility regime measurements (Morse, 1986) as $\tau_c = K\Delta H_0[(h_0/h_{-1})^{1/2} - 1]$, where ΔH_0 is the peak-to-peak linewidth of the central line of the EPR spectrum (in Gauss), and h_0 and h_{-1} are the peak amplitudes of the central and high-field lines. K depends on the magnetic field and on the anisotropy of both the g factor

and the hyperfine interaction (Kivelson, 1972), and should be determined for each spin label. However, this is not necessary in our case, as K cancels in the relative microviscosity determinations.

The intensity of the signal, in arbitrary units, is quantified as $I_0 = h_0(\Delta H_0)^2$ and normalised to microwave power, modulation amplitude, spectrometer gain and sample volume. For each set of samples (original, quenched and F&T), the reported intensities are normalised to the original one. The resultant values indicate the amount of unquenched spin label relative to that of the original sample.

2.6. Study of the hydrophobic region

The apparent order parameter (S_{app}) at different levels of the hydrophobic region is studied with the amphiphilic lipid-like labels n-SASL. They were incorporated to the samples as described previously and they are located preferentially in the hydrocarbon region with their long axes parallel to the acyl chains of the lipid molecules (Griffith and Jost, 1976). The polarity at the level of the end segments of the acyl chains is evaluated from the spectra of 16-SASL.

2.6.1. Analysis of the EPR spectra

The spectra of 5- and 12-SASL correspond to a regime of anisotropic movements with the axis of symmetry perpendicular to the aggregate surface. Then, the outer and inner hyperfine splittings $2A_{max}$ and $2A_{min}$ in the SASL spectra allow us to calculate the apparent (molecular) order parameter S_{app} (Griffith and Jost, 1976) as:

$$S_{app} = (1/k_0)(\bar{A}_{//} - \bar{A}_{\perp})/[A^c_{zz} - \tfrac{1}{2}(A^c_{xx} + A^c_{yy})]$$

where

$$\bar{A}_{//} = A_{max},\ \bar{A}_{\perp} = A_{min} + 1.4(1 - S_0),\ \text{with}$$

$$S_0 = (A_{max} - A_{min})/\left[A^c_{zz} - \frac{1}{2}(A^c_{xx} + A^c_{yy})\right],$$

$$A^c_0 = \frac{1}{3}(A^c_{zz} + A^c_{xx} + A^c_{yy}),$$

$$A_0 = \frac{1}{3}(\bar{A}_{//} + 2\bar{A}_{\perp}),\ \text{and}\ k_0 = A_0/A^c_0.$$

The parameters $A^c_{zz} = 32.9$ G, $A^c_{xx} = 5.9$ G and $A^c_{yy} = 5.4$ G, are the single crystal values of the ^{14}N hyperfine coupling tensor (Griffith and Jost, 1976). The above calculations were applied to 5-, 12- and 16-SASL spectra for comparative purposes, although 16-SASL shows almost isotropic spectra. This fact allows us to use the isotropic hyperfine constant A_0 obtained from 16-SASL spectra as an estimator of polarity changes in the hydrophobic zone upon Chol addition.

3. Results

3.1. Characterisation of the aggregates

3.1.1. Pure gangliosides

Fig. 1 shows the EPR spectra of TA in dispersions of pure gangliosides, G_{M1a} (a) and TBG (b), including in each case the original, quenched and F&T samples. For each of these spectra, the intensity of the signal I_0, the isotropic hyperfine constant A_0 and the relative microviscosity η_r were calculated as described in Section 2. As a reference, the spectrum of TA dissolved in the same buffer employed to swell the lipids yields $A_0 = 16.90$ G. In this case, $\eta_r = 1$ (by definition).

From the spectrum of the original sample of pure G_{M1a} (Fig. 1(a), original), we obtained $A_0 = 16.90$ G and $\eta_r = 2.8$, consistent with an aqueous medium of increased viscosity. In the quenched sample (Fig. 1(a), quenched), the intensity of the signal is approximately 6% of the original one, the hyperfine constant ($A_0 = 16.20$ G) corresponds to a less polar environment than that detected by TA in the original sample, and the microviscosity value ($\eta_r = 33.0$) indicates more restricted motions. The spectrum after F&T yields parameters very similar to those of the quenched sample, indicating that the original G_{M1a} structures do not enclose water. Comparison of this spectrum (magnified in Fig. 2(b)) with that of the residual signal corresponding to TA and FCN in pure buffer (Fig. 2(a)) in the same scale shows that their amplitudes and lineshapes are completely different. Therefore, the EPR signals of the quenched and F&T samples are not originated in an incomplete quenching but they probably arise on TA

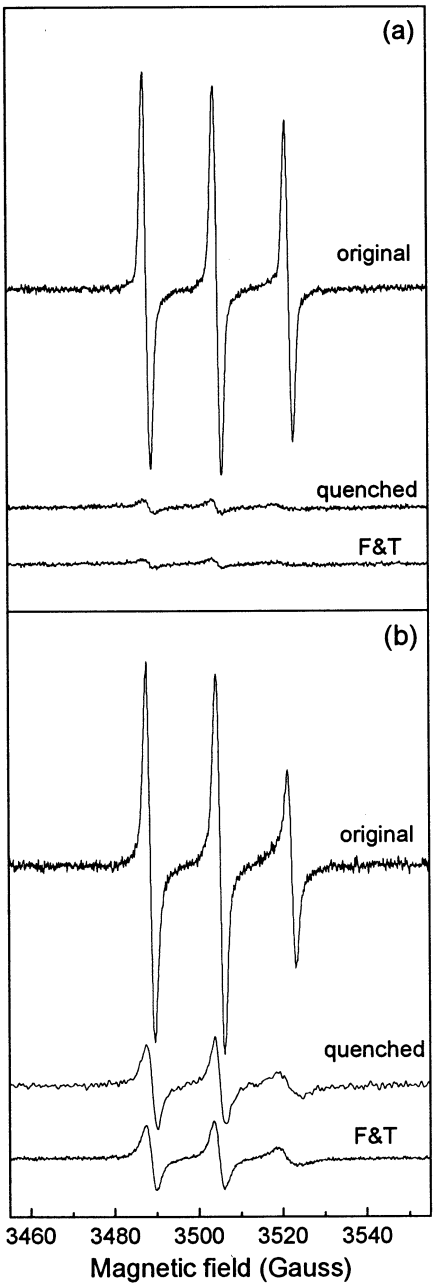

Fig. 1. EPR spectra of Tempamine in pure ganglioside water dispersions. (a) $G_{M1a,}$ (b) TBG. 'Original' and 'Quenched' samples denote the situations before and after the addition of FCN (quencher), respectively. 'F&T' corresponds to those quenched samples submitted to the freeze and thaw procedure (see Section 2). Microwave frequency is 9.84 GHz.

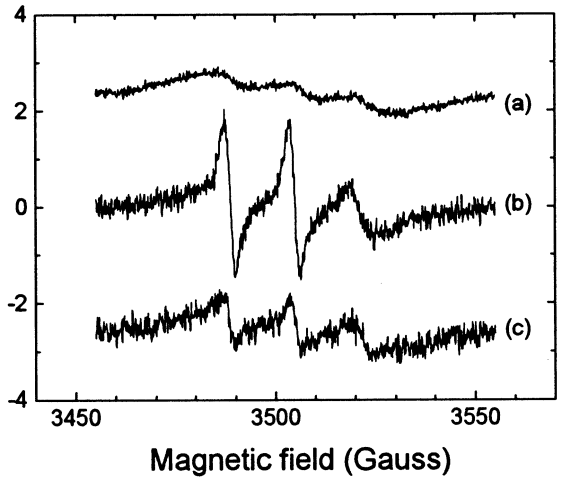

Fig. 2. EPR spectra obtained after quenching the TA spin label (1 mM) with potassium ferricyanide (FCN) up to a final FCN concentration of 65 mM (a) in pure buffer, (b) in pure G_{M1a} dispersions, after a further freeze-thaw procedure (note the differences both in shape and amplitude with the residual spectrum in (a)), (c) in G_{M1a}/Chol dispersions ($x_{Chol} = 0.3$) also after freeze-thaw. Note the reduction in amplitude when compared to (b).

molecules trapped by electrostatic interactions in protected sites among the negatively charged ganglioside headgroups. The inefficiency of FCN to quench these TA molecules is probably due to the electrostatic repulsion between the FCN anion and the ganglioside headgroups, although steric limitations could also play a role in this effect. The values of the relative intensities I_0/I_{0orig} (normalised to those of the corresponding original samples), the hyperfine constant A_0, and the relative microviscosity η_r are shown in the bar diagram of Fig. 3. For each value of x_{Chol}, the three bars from left to right represent the values measured in the original (light grey), quenched (dark grey) and F&T samples (white), respectively. The horizontal dotted line at $A_0 = 16.90$ G corresponding to TA dissolved in buffer is given as a reference.

In the case of pure TBG (natural mixture without Chol, Fig. 1b), the EPR spectrum of the original sample indicates a more viscous solution ($\eta_r = 13.3$), and a somewhat less polar environment ($A_0 = 16.76$ G) than in the original sample of G_{M1a} (Fig. 3). Quenching gives a reduced EPR.

signal, but its relative intensity is larger than in G_{M1a}, representing 35% of the original spectrumBesides, as it can be appreciated by comparing Fig. 1(b) (quenched) and Fig. 2(a), the lineshape and intensity of the quenched spectrum are again completely different from the residual signal of TA quenched in pure buffer. The values $A_0 = 16.05$ G and $\eta_r = 39$ indicate that TA is in a regime of restricted (though isotropic) motions, in a less polar environment than the bulk of the original sample. The spectrum remains almost unchanged after F&T. Thus, once again it is assumed that the EPR signal of the quenched sample comes only from the TA hidden among the ganglioside headgroups in a micellar structure.

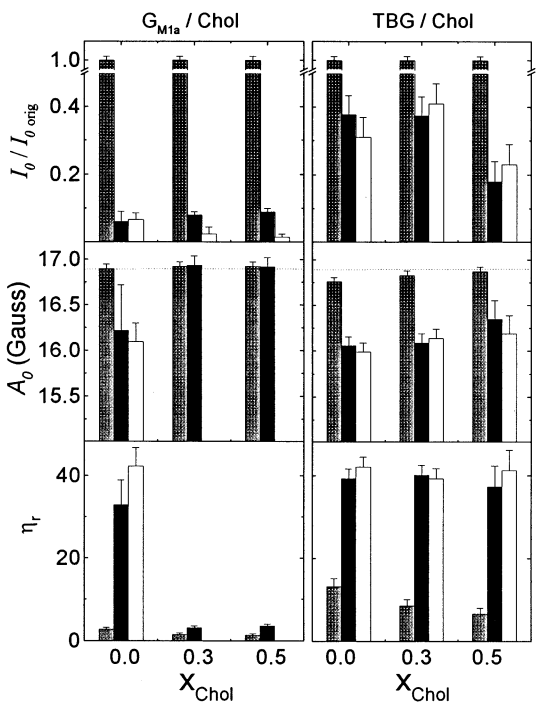

Fig. 3. Parameters extracted from EPR spectra of Tempamine labelled samples of G_{M1a}/Chol and TBG/Chol, shown as functions of cholesterol molar ratio. Upper panels: relative EPR intensity $I_0/I_{0\ orig}$, where $I_{0\ orig}$ corresponds in each case to the original sample. Intermediate panels: isotropic hyperfine constant A_0. Bottom panels: relative microviscosity η_r. The light grey, dark grey, and white bars correspond to the original, quenched, and F&T samples, respectively. In the intermediate panels, the horizontal dotted line at $A_0 = 16.90$ G corresponds to TA dissolved in buffer, for which $\eta_r = 1$. Values of A_0 and η_r are not given for F&T G_{M1a}/Chol samples at $x_{chol} = 0.3$ and 0.5, as their EPR spectra are poorly defined due to their small amplitude (see Fig. 2(c)).

3.1.2. Ganglioside/cholesterol mixtures

Fig. 4 shows the EPR spectra of TA obtained in ganglioside/Chol dispersions with $x_{Chol} = 0.3$for G_{M1a} (Fig. 4(a)), and TBG (Fig. 4(b)), respectively. Some important facts must be remarked: the intensity of the G_{M1a}/Chol spectrum is greatly reduced after quenching, but its shape, and the values of η_r and A_0 (Fig. 3, left panels) are indicative of an isotropic, low viscosity, and high polarity medium. Evidently, in the quenched sample, there is TA surrounded by an aqueous environment that is not accessible to FCN. After F&T (Fig. 4(a), amplified in Fig. 2(c)) the resulting spin intensity is further decreased, being only a 2% of that corresponding to the original sample. In this case, the amplitude of the signal is only about twice that of the residual one (obtained for TA and FCN in pure buffer, Fig. 2(a)), and thus it is not possible to obtain reliable values for η_r and A_0. This negligible intensity after the F&T procedure indicates a complete equilibration of the inner and outer media. These results allow us to affirm that the mixture G_{M1a}/Chol with $x_{Chol} = 0.3$ self-assembles in vesicular structures with enclosed water, which is accessible to FCN only after the F&T process. The turbidity of the sample agrees with these results.

Fig. 4(b) shows the corresponding spectra for TBG/Chol, $x_{Chol} = 0.3$. In this case, the quenched spectrum yields A_0 and η_r values (Fig. 3, right panels) characteristic of an environment with lower polarity and higher microviscosity than the aqueous one. The F&T spectrum is practically indistinguishable from the quenched one, strongly suggesting that the structure of this mixture remains micellar. This fact is in agreement with the transparency of the sample.

Fig. 5(a) displays the spectra for G_{M1a}/Chol with $x_{Chol} = 0.5$. As it occurs with $x_{Chol} = 0.3$, the set of spectra is characteristic of vesicles, i.e. a quenched spectrum of high polarity and low microviscosity values, and an almost complete extinction of the signal after F&T.

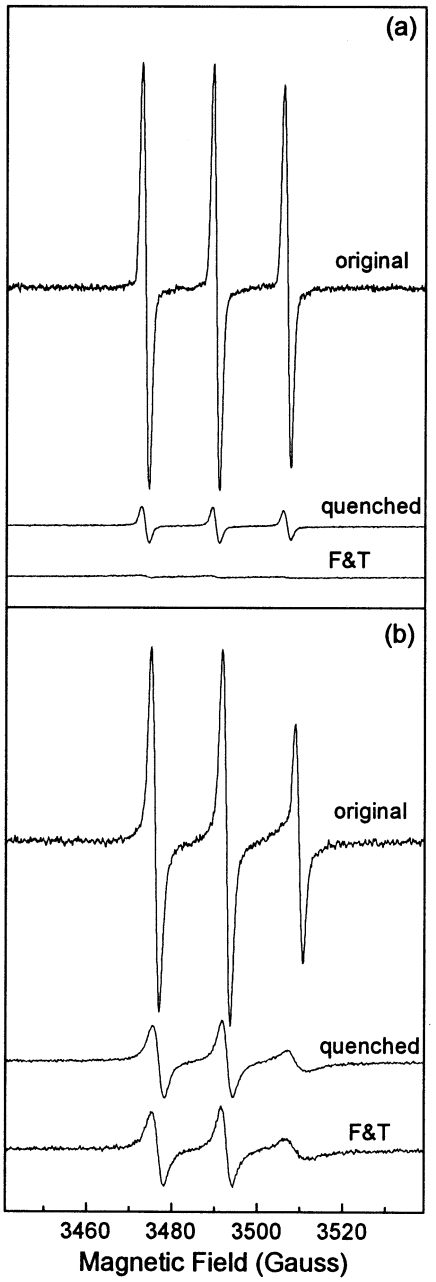

Fig. 4. EPR spectra of TA in ganglioside/Chol dispersions with $x_{Chol} = 0.3$. (a) G_{M1a}/Chol; (b) TBG/Chol. The labels have the same meanings as in Fig. 1. Microwave frequency is 9.80 GHz.

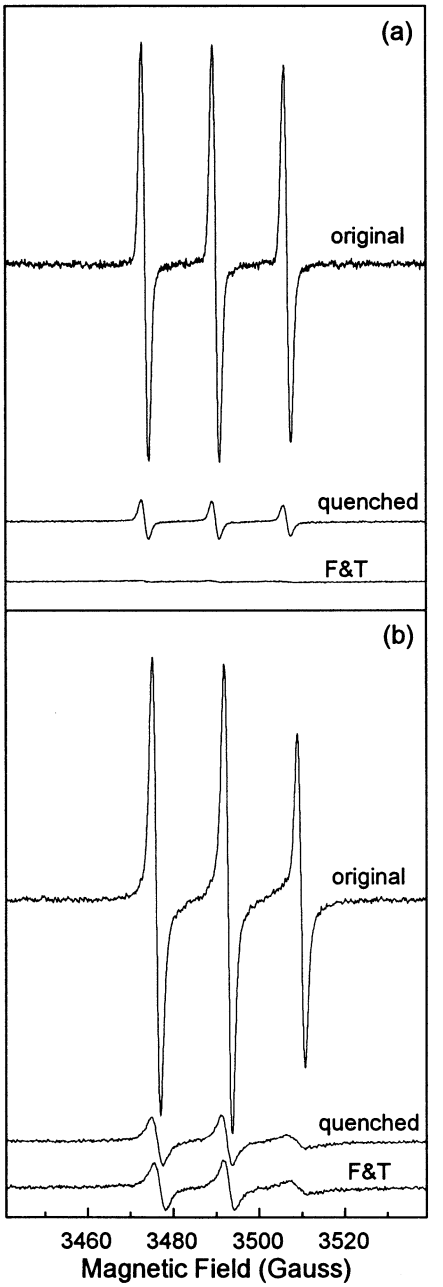

Fig. 5. EPR spectra of Tempamine in ganglioside/Chol dispersions with $x_{Chol} = 0.5$. (a) G_{M1a}/Chol; (b) TBG/Chol. The labels have the same meanings as in Fig. 1. Microwave frequency is 9.80 GHz.

In TBG/Chol, $x_{Chol} = 0.5$, the visual observation of small precipitates led us to consider the presence of large aggregates like vesicles or other extended structures. Nevertheless, the set of EPR

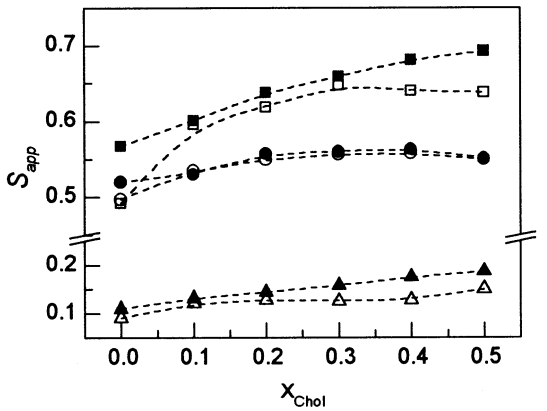

Fig. 6. Apparent order parameters calculated from the EPR spectra of SASL as a function of Chol molar ratio as explained in the text. Squares, 5-SASL; circles, 12-SASL; triangles, 16-SASL. Full symbols correspond to G_{M1a} mixtures, and open symbols to TBG mixtures.

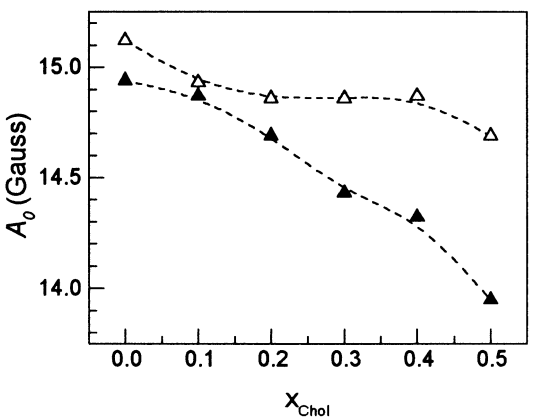

Fig. 7. Hyperfine isotropic values, representative of the polarity of the environment, extracted from the 16-SASL spectra, as a function of Chol molar ratio. Full triangles correspond to G_{M1a} mixtures, and open triangles to TBG mixtures.

spectra (Fig. 5(b)) is similar to that of $x_{Chol} = 0.3$, not reflecting the existence of well behaved water-enclosing vesicles. The presence of 'leaky vesicles' permeable to the FCN anion might be proposed. However, there are no significant differences between quenched and F&T spectra (Fig. 5(b)), and the A_0 and η_r values show only minute differences with respect to those corresponding to $x_{Chol} = 0.0$ and $x_{Chol} = 0.3$ (Fig. 3). These facts suggest that the aggregates formed by TBG/Chol at $x_{Chol} = 0.5$ are mostly large micelles.

3.2. Study of the hydrophobic region

The apparent order parameter S_{app} calculated from the SASL spectra as described in Section 2, provides a measure of the straightening of the acyl chains (Griffith and Jost, 1976; Morrow et al., 1995). The calculated values of S_{app} are plotted in Fig. 6 as a function of Chol content. A steady increase in S_{app} is observed for both G_{M1a} and TBG mixtures at all levels of the acyl chains as x_{Chol} is increased up to $x_{Chol} = 0.3$. At higher Chol contents, S_{app} for TBG (all labels) and for G_{M1a} (12-SASL) remains almost constant, while S_{app} from 5- and 16-SASL in G_{M1a}/Chol mixtures increase.

The isotropic hyperfine constant A_0 can also be calculated as described previously for the SASL. The EPR spectra of 5- and 12-SASL at room temperature contain contributions from slow molecular motions. Thus, the apparent hyperfine splittings depend on the rates as well as on theamplitudes of motion, precluding a direct correlation with the polarity of the environment of the spin labelled chain segment. For 16-SASL the slow motional effects are likely to be absent due to the fast end chain motions, thus allowing for the estimation of a local polarity from the A_0 values (Schorn and Marsh, 1996). The plot of A_0 (16-SASL) as a function of x_{Chol} represents the evolution of the averaged polarity at the level of the end segments of the hydrocarbon chains. This plot is presented in Fig. 7, where it can be seen that G_{M1a}/Chol dispersions show a steady decrease in the polarity of the hydrophobic core as x_{Chol} is increased. This fact is consistent with the transition to bilayer structures, as will be discussed later. On the other hand, the polarity sensed by the sixteenth carbon in TBG mixtures shows an initial decrease followed by a plateau region, and the values are always higher than in G_{M1a} mixtures. As it will also be discussed later, this fact supports the hypothesis of preservation of the micellar structure in TBG/Chol dispersions.

4. Discussion

The results obtained using the hydrosoluble spin label TA allowed us to discriminate between micellar and vesicular aggregates. In agreement with previous works using static and dynamic light scattering and electron microscopy (Maggio, 1994; Sonnino et al., 1994; Cantù et al., 1997), the whole set of our data indicates that the aggregates formed by G_{M1a} and TBG without Chol do not enclose water, i.e. they are micelles. The values of $\eta_r > 1$ for the original samples of both G_{M1a} and TBG (light grey bars in the lower panels of Fig. 3, $x_{Chol} = 0.0$) indicate that, at the present lipid/water molar ratio (1:555), the microviscosity of the aqueous environment is increased due to the presence of gangliosides (Bach et al., 1982; Arnulphi et al., 1997). This effect is more noticeable for TBG. In series of gangliosides with hydrophobic portions of similar compositions, it was foundthat the extent of the polar headgroup is the main determinant of the curvature radius and thus of the kind of structures to be adopted. G_{M3}, the smallest headed monosialoganglioside, self-assembles in vesicles. The remaining gangliosides have headgroups of increasing complexity and extension, and despite the presence of a double hydrophobic tail, they are cone shaped and form micelles. The rigid and complex structure of sugar and sialic acid molecules determines that the surface of the assembled structures is not smooth, having a high degree of 'surface roughness' (Sonnino et al., 1994).

After quenching with FCN the EPR signal due to TA in the external buffer, aqueous spectra were obtained for G_{M1a}/Chol aggregates (Fig. 3, Fig. 4(a) and Fig. 5(a) (quenched)). After the F&T process, when the quencher is able to reach all the aqueous environments, the EPR spectrum has a nearly negligible intensity. Thus, the aqueous environment sensed by TA in quenched G_{M1a}/Chol samples (before the F&T process) should only be attributed to water enclosed by vesicles. The observation of turbidity in these samples, which increases with Chol content, supports the formation of vesicles.

It is interesting to remark that Chol incorporation as a 30% molar of total lipids drives the transition from micellar to vesicular structures in G_{M1a} mixtures, but it does not cause such effects in those of TBG, which undoubtedly remain as micelles at $x_{Chol} = 0.3$. At $x_{Chol} = 0.5$, TBG/Chol samples show a slight turbidity which could onlybe related to the formation of large non-spherical micelles or leaky vesicles, as EPR data do not support the formation of sealed structures enclosing water. Instead, G_{M1a}/Chol samples with $x_{Chol} = 0.5$ give again clear evidence of vesicular structures.

Further experimental manifestation of the micelle-vesicle transition for G_{M1a}/Chol aggregates come from the stearic acid labels (SASL). The apparent order parameter S_{app} (Fig. 6) increases steadily in the entire range of Chol concentrations in G_{M1a}/Chol dispersions (except for the 12-SASL case, where it saturates). Instead, in TBG/Chol, S_{app} for the three SASL has a plateau region beginning near $x_{Chol} = 0.3$, beyond which only slight variations are observed. The order parameter gives information about the angular amplitude of motion of the labelled chain segment. The increase of S_{app} reflects a restriction of the *trans-gauche* isomerism and the consequent straightening of the hydrocarbon chains (Morrow et al., 1995). This fact, together with the micelle to vesicle transition, is pictorially represented in Fig. 8. The 'ideal' fully extended (all-trans) conformation of all the acyl chains ($S_{app} = 1$) could only be realised when the chains have the same available transverse area at all depths of the hydrophobic core (Gruen, 1985). In that case, the shape associated with the molecule is a cylinder and the structure adopted should be a planar bilayer (Fig. 8(b)). In a micelle, instead, the associated molecular shape is a cone, and the available transverse area for a chain decreases as the centre of the aggregate is approached (Fig. 8(a)). Consequently, the average number of gauche bonds in the final segments of the chains increases notably from bilayers to micelles (Gruen, 1985). As a result, the chain straightening caused by Chol molecules has an upper limit imposed by steric hindrances in the case of micellar structures, but not in bilayer structures. Thus, the steady increase in S_{app} values with Chol addition supports the transition from micelles to vesicles for mixtures G_{M1a}/Chol, and the plateau observed in S_{app} val-

ues for TBG/Chol mixtures is consistent with the preservation of the micellar structure.

The changes in the polarity of the environment to which the end segments of the acyl chains are exposed, evaluated from the hyperfine constant of 16-SASL (Fig. 7) reinforce our previous discussion. In G_{M1a}/Chol structures, the polarity decreases steadily upon x_{Chol} increase (A_0 varies from 14.95 to 13.90 G), while in TBG/Chol the polarity shows higher values that vary very little with x_{Chol} (A_0 from 15.10 to 14.80 G). These increased polarity values at the level of the 16th carbon in TBG/Chol may be interpreted in two ways, both related to the reduced order parameter. By one side, the disorder would facilitate water penetration into the hydrophobic core, and by the other, fluctuations of the 16-SASL end-chain into regions of greater polarity could be increased. This last possibility has been considered and discarded for bilayers of phosphatidylcholine (Ge and Freed, 1998), but it may be operative in ganglioside micellar structures. As in G_{M1a}/Chol mixtures the addition of Chol causes a phase transition from micelles to vesicles, the decrease of polarity for the 16-SASL with increasing values of x_{Chol} is consistent with both possibilities mentioned above. By one side, it agrees with the reduction of water penetration into the hydrophobic core, and by the other side it is consistent with the detected transition to vesicles with progressive chain straightening that forces the end segments of the lipid chain to be confined into the hydrophobic core (Gruen, 1985). The larger and almost constant polarity measured in the 16-SASL environment in TBG/Chol mixtures could be explained by the persistence of the micellar structures, although it is also compatible with the presence of aggregates more permeable to water than the G_{M1a}/Chol ones.

As gangliosides are anionic lipids, it can be argued that the increase in ionic strength upon potassium ferricyanide addition during the quenching procedure could promote by itself the observed changes in the shape of the aggregates. However, gangliosides are different from common anionic lipids, as ganglioside micellar dimensions are mainly determined by the steric hindrance of the complex sugar headgroups at the water-micelle interface, and not by the electrostatic repulsion of the headgroups themselves (Professor M. Corti, personal communication). It has been verified experimentally that the G_{M1a} micelles do not change weight or shape on NaCl addition up to at least 100 mM (Corti and Cantù, 1990). On the other hand, electrokinetic studies indicate that monovalent cations do not bind significantly to G_{M1a}, G_{D1a}, or G_{T1} (McDaniel et al., 1986). Thus, the modifications in the ionic strength of the suspending medium, which are essential to perform the quenching procedure, are not likely to be responsible for the micelle to vesicle transition detected in G_{M1a}/Chol aggregates. Besides, it should be emphasised that no transition occurs in absence of cholesterol. Thus, it is not the ionic strength per se the cause of the transition.

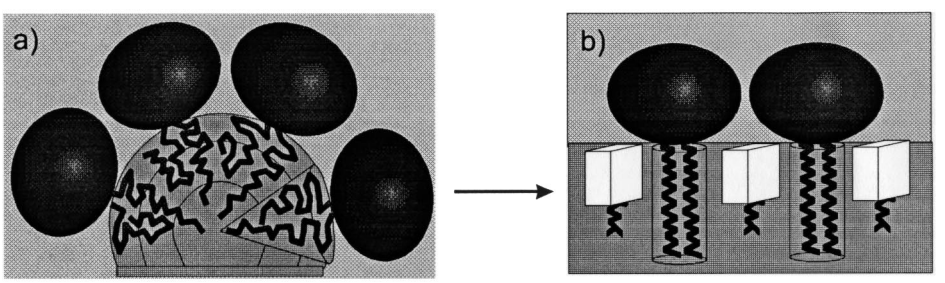

Fig. 8. Schematic representation of the role of cholesterol in promoting curvature changes in lipid structures. (a) Section of a micellar structure. The hydrocarbon chains are in a highly disordered state, due to the limited available space toward the centre of the structure. (b) Transversal section of a lipid structure of infinite curvature radius (air–water interface or vesicle hemilayer) formed upon Chol incorporation. Chol molecules act as walls separating the hydrocarbon chains, restricting trans-gauche isomerisations and promoting the all-trans extended state.

4.1. Origin of the EPR signal of the hydrosoluble spin label in freeze-thawed samples

In order to interpret the intensities of the remaining EPR spectra of TA obtained after quenching and freeze-thaw (Fig. 3, white bars in upper panels), two facts should be taken into account. First, TA does not partition into lipids, and second, FCN is not a radical scavenger, but only a 'line broadening', fast relaxing agent, which quenches reversibly the EPR signal of those spin labels in its close proximity (Morse, 1986). If a TA molecule migrates to sites not reachable by FCN, its EPR signal reappears. Thus, the quenching efficiency depends only on local FCN concentration. Electrostatic interactions should play an important role in this process. At the working pH value, TA is positively charged, and gangliosides bear negative charges in their headgroups due to the sialic acid moieties. The resulting attractive interaction would explain the penetration of TA into 'protected sites': windings and holes at the surface of the ganglioside aggregates (Cantù et al., 1997; Hirai and Takizawa, 1998). In contrast, FCN, bearing a charge -3, would be repelled from the surface, being unable to quench the EPR signal from TA into the protected sites. It is reasonable to expect that the number and size of these protected sites should depend on the curvature radius, being more important in micelles than in vesicles. Also it is expected that they should be more important in TBG micelles than in G_{M1a} ones, due to the inhomogeneity in headgroup sizes and the larger electrostatic effects present in the former (the mean charge per lipid molecule is -1.98 in TBG versus -1 in G_{M1a}).

The above reasoning can explain our experimental results, which show that the EPR spectrum of TA in the F&T sample of pure TBG has a larger relative intensity than that of the F&T sample of pure G_{M1a} (Figs. 1 and 3). Moreover, the intensities of the F&T spectra in mixtures G_{M1a}/Chol (vesicles) are negligible, while those in TBG/Chol mixtures remain with an appreciable intensity, consistent with less packed headgroups in structures of smaller radius of curvature.

The protected sites capable to enclose TA molecules seem to be related to the recently reported cavities existing in the ganglioside headgroups, which are able to enclose water molecules. These cavities are larger in disialogangliosides than in G_{M1a} structures (Hirai and Takizawa, 1998). The measured polarity in our protected sites (hyperfine constant around 16.1 G) is lower than that corresponding to free water or bulk buffer, although higher than that of a hydrocarbon chains environment. This fact seems reasonable considering that the sugars in the headgroups should generate a micropolarity approaching that of alcohols (lower than that of water), even when a few water molecules could share a hole with a TA molecule. The relative microviscosity sensed by TA in these sites varies between 35 and 40, for TBG, TBG/Chol and pure G_{M1a} aggregates. Although this is a high viscosity, the spectra correspond to isotropically rotating labels (Fig. 1, Fig. 2(b), Fig. 4(b) and Fig. 5(b)), showing that TA is not immobilised into the protected sites.

As the hydration process leads the system to a thermodynamically stable phase, it is expected that the F&T procedure, which causes the rupture and re-assemblage of the structures, would return the system to equilibrium preserving the size and number of protected sites. This assumption is confirmed by our results, as the quenched and F&T spectra in the case of micelles yield very similar parameters (Fig. 3, G_{M1a} at $x_{chol} = 0.0$ and TBG at all x_{chol} values). In the case of G_{M1a}/Chol aggregates, the quenched TA spectra are clearly attributable to a water environment, with hyperfine constant of 16.9 G, and relative microviscosity ~ 3. The F&T spectra of G_{M1a}/Chol have a negligible relative intensity, and they are strikingly different from the untreated quenched ones, discarding the possibility that the latter were originated in the protected sites discussed in the preceding paragraph. Thus, it is confirmed that truly vesicular structures are formed in G_{M1a}/Chol mixtures for $x_{Chol} \geq 0.3$.

The intensity of the F&T spectra in G_{M1a}/Chol decreases considerably from $x_{Chol} = 0.0$ to 0.3 and 0.5 (Fig. 3, left upper panel, white bars). This intensity reduction is consistent with an increased curvature radius, promoted by Chol incorporation, which allows for closer packing of G_{M1a} headgroups (Fig. 8). The straightening of the acyl

chains support this fact. These changes cooperate to produce a compact surface in which there are no holes to keep TA molecules protected from the FCN anions. This finding can be related with a recent report (Bagatolli et al., 1998) suggesting that water penetration in ganglioside structures is decreased by Chol addition.

5. Conclusions

We have reported a set of experimental data that helps to characterise the structures adopted by ganglioside/Cholesterol mixtures dispersed in water. While pure ganglioside dispersions are micellar, the addition of Chol to the monosialoganglioside G_{M1a} induces the formation of vesicles, clearly detected by our EPR studies from $x_{Chol} = 0.3$ and up. In contrast, the micellar structure adopted by the natural mixture of brain gangliosides TBG is maintained upon Chol incorporation up to at least $x_{Chol} = 0.3$. At higher proportions of Chol, the TBG/Chol samples become turbid indicating the formation of larger aggregates. Nevertheless, the EPR data are conclusive in showing that whatever they are, these aggregates are not able to enclose water.

The changes in the topology of the aggregates are also manifest in the behaviour at the level of the hydrophobic portion. The straightening in the acyl chains induced by cholesterol is more pronounced in mixtures with G_{M1a} than with TBG. Besides, polarity estimations suggest that the end portion of the acyl chains in G_{M1a}/Chol mixtures can be immersed more deeply in the hydrophobic core that in TBG/Chol mixtures, indicating that the available volume for the hydrocarbon chains is modulated by the curvature of the aggregates.

The transition from micelles to vesicles reported here might be relevant in the context of recent studies that indicate that some membrane proteins are unable to function in the absence of certain non-bilayer forming lipids. Although the mechanism by which the lipid properties affect protein behaviour is not understood, it has been suggested that some proteins must be sensitive to membrane curvature (Dan and Safran, 1998). In this sense, the mixtures of lipids used in this work seem very suitable to study the dependence of protein performance on spontaneous curvature of the membrane. Moreover, the constituents of the mixturesare those found in the dynamic clusters that serve as platforms for the attachment of proteins (Simons and Ikonen, 1997).

Acknowledgements

The authors are very grateful to Professor G.G. Montich for his help and advice in spin labelled sample preparation and to Professor M. Corti for his personal communication. This work was supported by Fundación Antorchas, CONICET (Proj. 4807, PEI 230/97), ANPCYT (PMT-PICT 0055, PMT-PICT 4066), CONICOR, SeCyT-UNC and Universidad Nacional del Litoral (CAI + D 53/96). P.R. Levstein, G.D. Fidelio and A.M. Gennaro are members of the research career of CONICET, Argentina, and M.M. Pincelli held a CONICET fellowship during the execution of this work.

References

Arnulphi, C., Levstein, P.R., Ramia, M.E., Martín, C.A., Fidelio, G.D., 1997. Ganglioside hydration study by ^{2}H-NMR: dependence on temperature and water/lipid ratio. J. Lipid Res. 38, 1412–1420.

Bach, D., Sela, B., Miller, I.R., 1982. Compositional aspects of lipid hydration. Chem. Phys. Lipids 31, 381–394.

Bagatolli, L.A., Gratton, E., Fidelio, G.D., 1998. Water dynamics in glycosphingolipid aggregates studied by LAURDAN fluorescence. Biophys. J. 75, 331–341.

Cantù, L., Corti, M., Del Favero, E., Raudino, A., 1997. Physical aspects figure of non-ideal mixing of amphiphilic molecules in solution: the interesting case of gangliosides. J. Phys. Condens. Matter 9, 5033–5055.

Carnie, S., Israelachvili, J.N., Pailthorpe, B.A., 1979. Lipid packing and transbilayer asymmetries of mixed lipid vesicles. Biochim. Biophys. Acta 554, 340–357.

Castanho, M.A.R.B., Brown, W., Prieto, M.J.E., 1992. Rodlike cholesterol micelles in aqueous solution studied using polarized and depolarized dynamic light scattering. Biophys. J. 63, 1455–1461.

Corti, M., Cantù, L., 1990. Application of scattering techniques in the domain of amphiphiles. Adv. Colloid Interface Sci. 32, 151–166.

Dan, N., Safran, S.A., 1998. Effect of lipid characteristics on

the structure of transmembrane proteins. Biophys. J. 75, 1410–1414.

Fidelio, G.D., Ariga, T., Maggio, B., 1991. Molecular parameters of gangliosides in monolayers: comprehensive evaluation of suitable purification procedures. J. Biochem. 110, 12–16.

Ge, M., Freed, J.H., 1998. Polarity profiles in oriented and dispersed phosphatidylcholine bilayers are different: an electron spin resonance study. Biophys. J. 74, 910–917.

Gennaro, A.M., Luquita, A., Rasia, M., 1996. Comparison between internal microviscosity of low-density erythrocytes and the microviscosity of hemoglobin solutions: an electron paramagnetic resonance study. Biophys. J. 71, 389–393.

Griffith, O.H., Jost, P.C., 1976. Spin labels in biological membranes. In: Berliner, L.J. (Ed.), Spin Labeling: Theory and Applications. Academic Press, New York, pp. 454–523.

Gruen, D.W.R., 1985. A model for the chains in amphiphilic aggregates. 2. Thermodynamic and experimental comparisons for aggregates of different shape and size. J. Phys. Chem. 89, 153–163.

Hirai, M., Takizawa, T., 1998. Intensive extrusion and occlusion of water in ganglioside micelles with thermal reversibility. Biophys. J. 74, 3010–3014.

Israelachvili, J.N., 1991. Intermolecular and Surface Forces. Academic Press, New York, pp. 380–382.

Kivelson, D., 1972. Electron spin relaxation in liquids. Selected topics. In: Muus, L.T., Atkins, P.W. (Eds.), Electron Spin Relaxation in Liquids. Plenum, New York, pp. 213–227.

Kumar, V.V., Anderson, W.H., Thompson, E.W., Malewicz, B., Baumann, W.J., 1988. Asymmetry of lysophosphatidylcholine/cholesterol vesicles is sensitive to cholesterol modulation. Biochemistry 27, 393–398.

Ledeen, R.W., Hogan, E.L., Tettamanti, G., Yates, A.J., Yu, R.K. (Eds.), 1988. New Trends in Ganglioside Research: Neurochemical and Neuroregenative Aspects, vol. 14. Liviana Press, Padova.

Liu, Y.B., Chan, K.F., 1991. High-performance capillary electrophoresis of gangliosides. Electrophoresis 12, 402–408.

Maggio, B., 1994. The surface behaviour of glycosphingolipids in biomembranes: a new frontier of molecular ecology. Prog. Biophys. Molec. Biol. 62, 55–117.

Mayer, L.D., Hope, M.J., Cullis, P.R., Janoff, A.S., 1985. Solute distributions and trapping efficiencies observed in freeze-thawed multilamellar vesicles. Biochim. Biophys. Acta 817, 193–196.

McDaniel, R.V., Sharp, K., Brooks, D., McLaughlin, A.C., Winiski, A.P., Cafiso, D., McLaughlin, S., 1986. Electrokinetic and electrostatic properties of bilayers containing gangliosides GM1, GD1a, or GT1. Comparison with a non-linear theory. Biophys. J. 49, 741–752.

Morrow, M.R., Singh, D., Lu, D., Grant, D.W.M., 1995. Glycosphingolipid fatty acid arrangement in phospholipid bilayers: cholesterol effects. Biophys. J. 68, 179–186.

Morse, P.D., 1986. Determining intracellular viscosities from the rotational motion of spin labels. Methods Enzymol. 127, 239–249.

Perkins, W.R., Dause, R.B., Li, X., Franklin, J.C., Cabral-Lilly, D.J., Zha, Y., Dank, E.H., Mayhew, E., Janoff, A.S., 1997. Combination of antitumor ether lipid with lipids of complementary molecular shapes reduces its hemolytic activity. Biochim. Biophys. Acta 1327, 61–68.

Pincelli, M.M., Levstein, P.R., Martín, C.A., Fidelio, G.D., 1998. Cholesterol-induced stablilization of lamellar structures in ganglioside-containing lipid aggregates. A ^{31}P-NMR study. Chem. Phys. Lipids 94, 109–118.

Schorn, K., Marsh, D., 1996. Lipid chain dynamics and molecular location of diacylglycerol in hydrated binary mixtures with phosphatidylcholine: spin-label ESR studies. Biochemistry 35, 3831–3836.

Simons, K., Ikonen, E., 1997. Functional rafts in cell membranes. Nature 387, 569–572.

Sonnino, S., Cantù, L., Corti, M., Acquotti, D., Venerando, B., 1994. Aggregative properties of gangliosides in solution. Chem. Phys. Lipids 71, 21–45.

Sunamoto, J., Akiyosi, K., Kihara, T., Endo, M., 1992. A water soluble spin probe newly developed for liposomal studies. Bull. Chem. Soc. Jpn. 65, 1041–1046.

Tettamanti, G., Masserini, M., 1987. Gangliosides and the transfer of information through the plasma membrane. In: Bertoli, E., Chapman, D., Cambria, A., Scapagnini, U. (Eds.), Biomembrane and Receptor Mechanisms. Fidia Research Series, vol. 7. Liviana Press, Padova, pp. 223–260.

Van der Meer, B.W., 1993. Fluidity, dynamics and order. In: Shinitsky, M. (Ed.), Biomembranes. Physical Aspects. VCH, Weinheim, pp. 97–158.

Wertz, J.E., Bolton, J.R., 1972. Electron Spin Resonance.Elemental Theory and Practical Applications. McGraw-Hill, 497 pp, New York.